# Profiles of the Compton Band from Lithium*

ALEXANDER THEODOSSIOU AND PETROS VOSNIDIS
*Physics Department, Athens University, Athens, Greece*
(Received 13 December 1965)

Measurements are reported on the Compton profile from Li for the Cr $K\beta$ radiation for scattering angles 10°, 18°, 32°, and 45°. As the momentum transferred to the recoil electron depends on the scattering angle $\varphi$, a critical value $\varphi_0$ is found beyond which all the valence electrons contribute to the scattering. For the case $\varphi > \varphi_0$ the profile is known to be parabolic, while for $\varphi < \varphi_0$ the elementary theory predicts that the profile consists of a parabolic part which is continued by an inclined straight line terminating at the position of the unmodified line. Our effort was mainly concentrated on scattering angles below $\varphi_0$. Because of experimental errors and also the nonmonochromatic nature of the primary radiation, it is difficult to determine the exact shape of the profile. But there is a discrepancy with the profiles calculated both by the Hartree-Fock approximation (noninteracting free-electron gas) and in the random-phase approximation (with Coulomb interaction). For scattering angle 45°, i.e., larger than $\varphi_0$, the measured half-width is 28±5 eV, of the same order of magnitude as the value obtained by theory.

## INTRODUCTION

WHEN x rays fall on a crystalline material, the scattered radiation appears mainly along certain directions, where the Debye-Scherrer lines are detected. This scattering is a result of interference of waves reflected by the various sets of crystal planes. In this scattering, no change of the wavelength takes place.

In addition to the Debye-Scherrer lines, much weaker scattering appears in all directions. The spectral analysis of this diffuse radiation proves that it consists of two components, one of which has practically unmodified wavelength (Rayleigh line) and the other a longer wavelength (modified or Compton line). The wavelength shift $\Delta\lambda$ of the Compton component for a stationary free electron depends on the scattering angle $\varphi$ according to the formula

$$\Delta\lambda = (h/mc)(1-\cos\varphi) .$$

The unmodified component is due to the interaction between photons and elastic waves of the scatterer, in which the energy of the photon may be changed by an amount equal to the energy of a created or absorbed phonon.

In the fictitious case of a stationary free electron, the Compton line would have strictly one frequency. The electrons actually are in motion, belonging either to a free atom or to a solid. This causes the modified line to spread out in both directions around the position of the Compton line and become a band. This was first explained as a Doppler effect, because of the analogy to the broadening of the spectral lines due to the thermal motion of the atoms of the light source. On the basis of this analogy, the broadening of the band is given by the formula

$$\delta\lambda = 2\lambda(v\cos\theta/c)\sin(\varphi/2) ,$$

where $v\cos\theta$ is the component of the electron velocity along the scattering vector. Therefore the maximum broadening is

$$\delta\lambda = 4\lambda(v/c)\sin(\varphi/2) ,$$

where $v$ represents the maximum electron velocity.

In addition to the broadening of the Compton band it is interesting to consider the intensity distribution within the band, that is to say, the profile of the modified band, because it is directly correlated with the velocity distribution of the electrons contributing to the scattering.

Theory predicts that the Compton profile depends on the energy transferred to the recoil electron. Hence the experiments which study the profile as a function of the scattering angle should be divided into classes depending on the energy transfer, and the interpretation should also proceed accordingly.

Measurements exist only for large energy transfers,[1] i.e., for large scattering angles. The objective was the determination of the profile of the Compton band or its half-width.

Many articles[2–5] deal with the theoretical computation of the profile and its half-width. In general, the formulae used is the following:

$$J(q) = \tfrac{1}{2}\int_q^\infty \frac{I(p)}{p}dp .$$

This gives the intensity of the Compton band as a function of wavelength. $I(p)$ is the momentum-distribution function, which can be obtained from the wave function of the electrons contributing to the scattering. In the case of solids (metals), the wave functions must be modified to account for the atomic interaction.

The large discrepancy between the calculation and the early measurements of Kappeler[6] ascribed to the

* This research was supported in part by the Royal Hellenic Research Foundation and by the European Research Office of the U. S. Army.

[1] J. W. M. Dumond, Rev. Mod. Phys. **5**, 1 (1933).
[2] W. E. Duncanson and C. A. Coulson, Proc. Phys. Soc. (London) **57**, 190 (1945).
[3] N. H. March, Proc. Phys. Soc. (London) **A67**, 9 (1954).
[4] B. Donovan and N. H. March, Proc. Phys. Soc. (London) **69**, 1249 (1956).
[5] G. E. Kilby, Proc. Phys. Soc. (London) **82**, 900 (1963).
[6] H. Kappeler, Ann. Physik **27**, 129 (1936).

inaccuracy of the momentum eigenfunction of the electrons. Recent measurements of Cooper, Leake, and Weiss,[7] show that the disagreement is not so large as formerly assumed.

For the case of small energy transfer, which is the object of the present work, no measurements have been made up to now. A suitable theory, which extends to the range of the present measurements, has been published by Ohmura and Machudaira[8] and deals with the change of the profile as a function of the scattering angle. They give two different approaches to the problem: (a) neglecting, and (b) taking into account the Coulomb correlation of the electrons. For both cases they give the differential cross section as a function of the quantity $(\lambda'-\lambda)/\lambda_c$, where $\lambda$, and $\lambda'$ are the incident and scattered wavelengths, and $\lambda_c$ is the Compton wavelength for stationary electrons. They find that the Coulomb effect is proportional to $k^{-2}$, where $k$ is the transferred momentum. This means that the Coulomb interaction is significant for small $k$, and hence should be of considerable interest in the range of the present measurements. The Compton spectrum, calculated for a noninteracting electron gas (Hartree-Fock approximation) shifts towards larger wavelength. This is explained by considering the plasma excitations (oscillation of the electron particle density) and the emission of a "plasmon" (plasma quantum), during the scattering of a photon.

## PRESENT WORK—THEORY

In the present work Compton profiles were measured for several scattering angles and compared with calculated profiles. The calculation refers to the valence electrons of the monovalent metals and neglects the contribution of the other electrons.

The intensity of the Compton scattering at a given energy shift is proportional to the product of the number of the initial and the final states compatible with the given energy difference, and under the condition that the initial state is occupied and the final state unoccupied. In the case of a metal scatterer, the shape of the Compton profile, near the unmodified line, depends on the density of states near the Fermi level and also on the shape of the Fermi surface. An analytical calculation of the shape of the profile can be made easily for the case of a spherical Fermi surface (free-electron gas), if we assume the transition probability to be constant. In a free-electron gas all states below the Fermi surface are occupied and all beyond it unoccupied

If we consider a Compton process, involving a given momentum transfer $\Delta p$, it is clear that of the total number $z$ of electrons in the Fermi sphere, only a part,

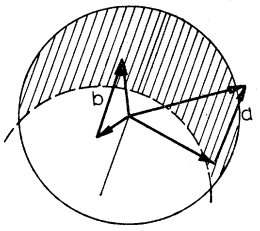


FIG. 1. (a) Process contributing to the Compton scattering and (b) noncontributing. The transferred momentum is the same in both cases.

equal to $z_{\text{eff}}$, contribute, that is, are brought to a final state outside the Fermi sphere after the scattering.

In Fig. 1 we have drawn the Fermi sphere and another one shifted by $\Delta p$. The number of effective electrons $z_{\text{eff}}$ corresponds to the electrons in the shaded part. We consider the cross section to be constant in the wavelength range over which the spectrum extends for a given scattering angle. The ratio $z_{\text{eff}}/z$ was calculated separately by Zener[9] and Debye[10] from geometrical considerations. They also gave the integrated intensity of the Compton band, without information on the profile.

For a given scattering angle $\varphi$, the momentum transferred to the recoil electron is, to a very good approximation,

$$\Delta p=(2h/\lambda)\sin(\varphi/2)\,.$$

Hence, because of the Pauli exclusion principle, only the electrons in the shaded part of the Fermi sphere contribute to the scattering. The shaded sphere is shifted exactly by $\Delta p$. Zener and Debye obtained for the ratio of the shaded part to the total volume of the sphere the formula

$$\frac{z_{\text{eff}}}{z}=\tfrac{3}{2}[(h/\lambda p_{\max})\sin(\tfrac{1}{2}\varphi)]-\tfrac{1}{2}[(h/\lambda p_{\max})\sin(\tfrac{1}{2}\varphi)]^3.$$

Beyond a certain value $\varphi_0$ of the scattering angle the ratio becomes unity. It can be easily shown that $\sin(\frac{1}{2}\varphi_0)=\lambda p_{\max}/h$, where $p_{\max}$, the maximum electron momentum, is calculated from

$$p_{\max}=[(N/V)(3/\pi)]^{1/3}\tfrac{1}{2}h.$$

$N/V$ is the density of the valence electrons. The value $\varphi_0$ corresponds to the case in which the common part of the spheres of Fig. 1 is limited to one point. In the quantity $(h/\lambda p_{\max})\sin(\frac{1}{2}\varphi)$, which appears in the horizontal axis of Fig. 2, we consider as variable only the scattering angle. The other quantities are fixed as soon as the wave length $\lambda$ and the material of the scatterer are chosen. We note that beyond the value $\varphi_0$, all the valence electrons contribute to the scattering, while for scattering angles $\varphi<\varphi_0$ the percentage becomes smaller with the scattering angle. The calculation of the intensity versus the energy shift gives a different shape of the profile if the scattering angle is

[7] Malcolm Cooper, J. A. Leake, and R. J. Weiss, Phil. Mag. **12**, 797 (1965).
[8] Y. Ohmura and N. Matsudaira, J. Phys. Soc. Japan **19**, 1355 (1964).
[9] C. Zener, Phys. Rev. **48**, 573 (1935).
[10] P. Debye, Physik. Z. **38**, 161 (1937).

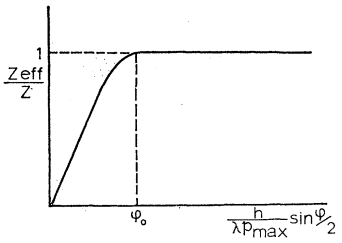


FIG. 2. Beyond angle $\varphi_0$ all the electrons contribute to the scattering and the shaded part of Fig. 1 extends to the whole sphere.

chosen to be smaller or larger than angle $\varphi_0$. For $\varphi > \varphi_0$ the profile is an inverse parabola, and for $\varphi < \varphi_0$, a part of the parabola towards the unmodified line is missing (see Appendix). The missing part is replaced by an inclinded straight line, that reaches the abscissa at the position of the unmodified line. Figure 3 illustrates the Compton profile for lithium and scattering angle $\varphi = 10°$. Both curves refer to strictly monochromatic radiation. Under experimental conditions the primary radiation is not monochromatic but exhibits a broadening; therefore a correction is necessary to allow comparison between measurements and theory. The purpose of these measurements is to verify the theoretically predicted profiles of the Compton band.

## EXPERIMENTAL SETUP

The spectrometer (Fig. 4) is a focusing instrument consisting of the following parts: the x-ray tube, the scatterer, the bent crystal and the detector (Geiger counter). All these parts of the apparatus were installed on an iron plate and care was taken so that the x-ray focus and the middle of the counter slit lay on the equatorial plane of the bent crystal. The crystal holder,[11] made of steel, was fixed on a circular disk of brass, the leveling of which was accomplished by three screws pressing aginst a second brass disk, which could be turned against a fixed graduate scale.

The counter was mounted on a slide[12] and could be rotated in the horizontal plane. The slide consists of two parallel steel plates. The upper one bears the rotatable two-cone system on which the slit and the counter are mounted. The two plates are kept apart with three spheres moving in two parallel grooves. This construction permits sliding of the upper plate with respect to the lower one.

In order to focus the x-ray beam, it is necessary that the slit in front of the detector lie on the Rowland circle

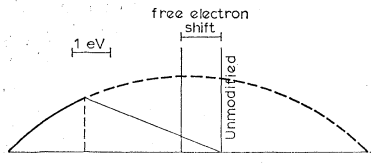


FIG. 3. Compton profile for $\varphi = 10°$ for a noninteracting electron gas.

[11] Thanks are due to Dr. Åke Nilsson (Uppsala) for providing the crystal holder.

[12] G. Brogren, thesis, Uppsala, 1949 (unpublished).

of diameter equal to the radius of curvature of the bent crystal.

Adjustment of the apparatus is facilitated by placing the base of the crystal and the slide at the two ends of a flat iron plate (A), which lies on the main iron plate and can be turned around a vertical axis through the center of the crystal. The position of this axis with respect to the scatterer depends on the scattering angle.

The motion of the slide was obtained by means of a micrometer screw, which was fixed on the upper plate of the slide. The orientation is arranged so that the slide moves tangentially to the Rowland circle. During the preliminary experiments, Cu $K\beta$ radiation was used because Cu targets can withstand higher power and because Cu radiation is not absorbed strongly in air. On the other hand, it has the disadvantage that the natural width of the line is large (6.3 eV), and becomes

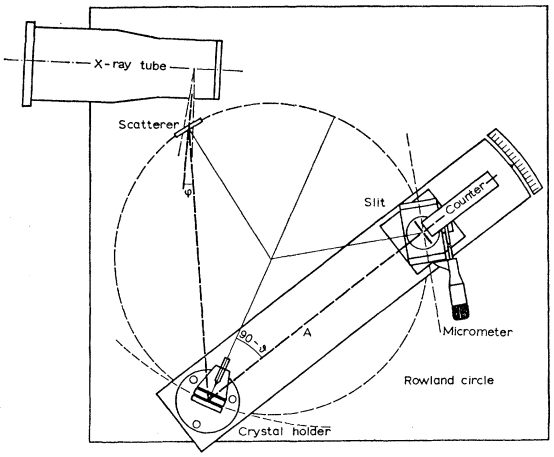


FIG. 4. The spectrometer. The scatterer in "transmission position."

even larger for experimental reasons (astigmatism of the spectrometer, width of the slit of the detector). The large width of the line prevents the resolution of the two components of the scattered radiation (Rayleigh and Compton), especially in the case of small scattering angles. From the latter point of view, a better choice is the use of Cr $K\beta$ radiation which has smaller natural width (3 eV). Unfortunately, the Cr tube used by us was of low power (only 300 W), giving a much weaker beam. Another disadvantage is that the Cr radiation is absorbed in air, losing half its intensity in 21 cm. To prevent this, the major paths of the beam were in evacuated tubes, closed with Mylar windows (not shown in Fig. 4). The bent crystal was a quartz plate 0.5 mm thick, cut in a $13\bar{4}0$ plane and provided by Steeg and Reuter, Bad Homburg, Germany. The fluorescence radiation of quartz is weak, and in addition the plane $13\bar{4}0$ has the advantage of very weak 2nd-order reflection. The crystal holder consists of two cylindrical surfaces, which have been carefully machined, determining a radius of curvature of 500 mm. However, this

does not necessarily mean that the part of the crystal corresponding to the window of the holder has the same radius.

In front of the crystal holder a trapezoidal piece of brass with a shutter is placed to ensure illumination only of the quartz crystal and not of the holder and also to limit what the counter slit "sees" to the area of the quartz crystal.

The characteristics of the equipment used were as follows: The x-ray tube with Cr target was operated at 24 kV and 12 mA. The stabilized high voltage and current were supplied by a Philips generator, type PW 1010. The actual size of the focus was $1\times10$ mm$^2$. This focus, as seen through the window, provides an optical spot of $1\times1$ mm$^2$. The Geiger counter had a counting efficiency of 60% for the wavelength of the line Cr $K\beta$. The mica window had an approximate thickness of 3 mg/cm$^2$. The width of the counter slit was 0.15 mm.

## ADJUSTMENT OF THE APPARATUS

For preliminary adjustment a beam of light was used. We removed the counter and in its position we placed a light source. The bent-crystal table was turned so that the image of the slit fell on the slit. The examination of the image gave initial information on the uniform bending of the crystal. Thereafter the bent-crystal table was turned by an angle equal to the supplement of the Bragg angle. This gave a coarse adjustment of the slit with respect the bent crystal. Then, the crystal was placed in the x-ray beam and the approximately correct orientation of the plate A found by using the proper (Bragg) angle cut from cardboard. The fine adjustment of the apparatus was attained with x rays. The leveling of the parts of the apparatus was checked by placing a piece of photographic film in front of the slit. The accurate measurement of the radius of the bent crystal was carried out by putting films at various distances from the crystal to find the focus position, which corresponds to the sharpest image of the x-ray beam. The distance between x-ray focus and crystal was kept equal to the length of the chord of the Rowland circle for our particular wavelength, which is also the distance between slit and bent crystal. The correct position of the slit with respect to the bent crystal was then found by measuring the counting rate while moving the detector along its slide. This was repeated for various positions of plate A around the position found by the cardboard. In this way we located the exact reading of the micrometer for maximum reflection. This adjustment was relatively easy because we used the primary beam, which is quite strong. For the present work, use was made of two different crystal holders. One had an opening with dimensions $5\times10$ mm$^2$. We also used another crystal holder with an opening twice as large, but the focusing was not satisfactory. We therefore decided to use the small holder, scarificing luminosity in favor of focusing. Better focusing means higher resolution which permits the detection of structural details. The x-ray adjustment gave a different position for the bent crystal by approximately 3° with respect to that found by the optical method. The discrepancy is due to an error in the cutting of the quartz crystal. Subsequently, the x-ray tube was placed so that the focus line was parallel to the Rowland circle, and the $K_\beta$ line was scanned in order to determine the half width. The value found was 3.14 eV, which is 1% larger than the value given in the literature.[13]

The process used in the measurements and in general for all scattered radiation was as follows: The counter slide was brought to a certain position, which was determined by the reading of the micrometer screw, and left there until it recorded a fixed number of counts. Then the slide was brought to the next position, and so on. The measured counting rates were plotted against the micrometer readings.

## SCATTERER

A polycrystalline block of lithium metal of 99% purity (Fluka AG, Switzerland) was used as scatterer. This is a monovalent metal which should follow the crude theory and should give a stronger Compton band than the other alkali metals. The purity of the sample is important, because a small concentration of foreign atoms would increase the absorption coefficient and hence decrease the quantity of the sample participating in the scattering. We determined the absorption coefficient of our sample, for Cr $K\beta$ wavelength, by measuring the counting rates when a lithium slab was placed in front of the counter slit and without it. The value found was $\mu=3.84$ cm$^{-1}$, which is about twice as large as the value appearing in the literature, indicating that the sample contained impurities.

## MEASUREMENTS AND RESULTS

An application of the formula for the critical angle for lithium at the wave length of Cr $K\beta(=2.08$ Å) gave the value $\varphi_0=43°$. We carried out measurements of the scattered radiation to determine the Compton profile for the following scattering angles: $\varphi=45°$, 32°, 18°, and 10°, mainly below the value $\varphi_0$. For the last two cases special precautions were necessary, so that the bent crystal did not "see" the exit hole of the x-ray tube. This was done with shields of lead, placed in convenient positions. These shields were also intended to minimize the volume of air which was seen from the crystal, so as to keep the air-scattered radiation low. For all scattering angles we made calculations to make sure that there were no Debye-Scherrer lines along the chosen directions. To decrease the background from stray radiation, a thick lead shield surrounded the counter.

[13] Åke Nilsson, Arkiv Fysik **6**, 513 (1953).

Before starting measurements, we calculated the Compton shift $\Delta\lambda$ and the width of the Compton band $\delta\lambda$, and we converted these quantitites to energy and then to units of length (mm) along the Rowland circle. In all cases the scattered radiation was measured with the scatterer in the "reflection position." In the case of $\varphi=10°$, measurements were repeated with the "transmission position" of the scatterer as shown in Fig. 4. The lithium sample in the reflection position was about 10 mm thick, while in the transmission position a slab 2 mm thick was found to be the optimum by a calculation based on the measured coefficient of absorption.

The experimental procedure was the following for all cases: After placing the scatterer in position in front of the x-ray tube and at a distance of 6.5 cm from the focus, we used an angle cut from cardboard to place the axis of the bent crystal in the desired direction of scattering. Then with the help of another cardboard we turned the plate A so that the bent crystal was approxi-

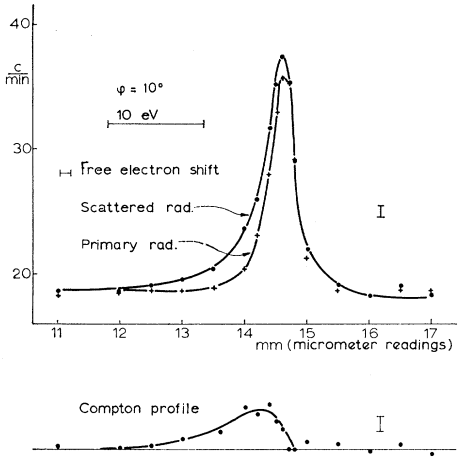


FIG. 5. Scattering on Li for $\varphi=10°$.

mately at the correct Bragg angle. Then, switching on the x-ray tube, we measured the counting rate for several angular positions of plate A. During these measurements the counter slit was set at a position of "maximum" reflection, determined in the previous experiment; hence in the present experiment the counting rate was a measure of the Rayleigh component of the scattered radiation. The curve plotted from these measurements (counting rate against the angular position of the plate A), as expected, showed a plateau, falling at both ends to the background level. From this curve we determined the proper angular position of plate A and also we had a safe indication of the adequacy of the length of the illuminated volume of Li along the Rowland circle. It is clear that if we consider the projection on the Rowland circle of the illuminated part of the scatterer, this projection must be long enough to allow sweeping of both components of the scattered radiation with the adjacent background. For

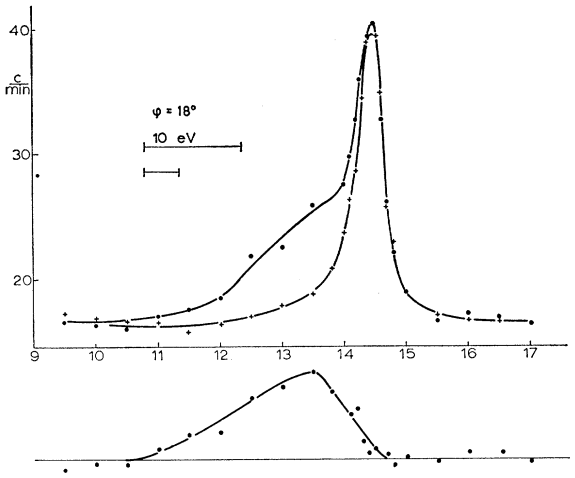


FIG. 6. Scattering on Li for $\varphi=18°$.

certain angles this condition could be improved by changing the orientation of the scatterer with respect to the incident beam, which increased the illuminated area. Figures 5, 6, 7, and 8 give the scattered radiation (counts/min) as it is scanned by the detector. The readings of the micrometer screw appear on the horizontal axis. In all figures we retain the same notation. The magnitude of the experimental errors is shown by small vertical lines.

## DUMMY EXPERIMENT

In almost all measured cases the two components, Rayleigh and Compton, overlap. To separate them, a dummy experiment had to be devised. In principle, various methods could be thought of. A first one was the use of the primary radiation by directly illuminating the spectrometer. The line obtained in this way cannot be used because of the different geometric conditions. When we illuminate the spectrometer directly we have a point source, while when we insert a scatterer, it serves as a source with large dimensions which causes

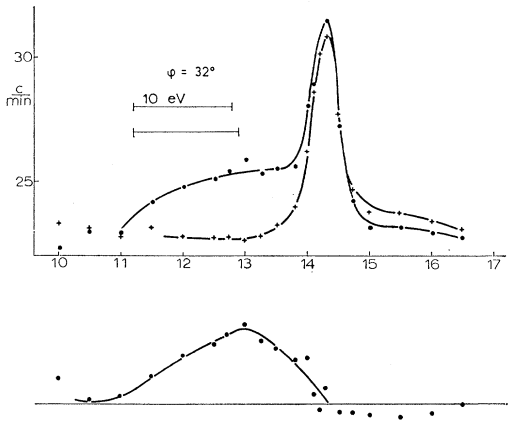


FIG. 7. Scattering on Li for $\varphi=32°$.

a broadening of the line. Another type of dummy experiment consisted in exchanging Li with a scatterer of another material, which would give a strong Rayleigh line with a negligible Compton component. The use of a copper plate was not satisfactory, since it gave low intensity of the Rayleigh line, because of the strong absorption of the Cr radiation. The use of Cr filings as a scatterer gave a very intense spectrum. This can be ascribed to the small absorption of the Cr $K\beta$ line in Cr because this region is on the long-wavelength side of the absorption edge (in contrast to Cr radiation in copper). The intensity of the Rayleigh line is increased also by the fluorescence radiation, excited in Cr by the hard range of the x-ray spectrum. The method of chromium filings in "reflection position" was applied for all dummy experiments with the following modification: The x-ray tube was turned to such a position that the scattering angle was large (25° for the case of $\varphi=10°$ and 40° for $\varphi=18°$ and 32°), without disturbing the other geometric conditions; i.e., the view of the scatterer

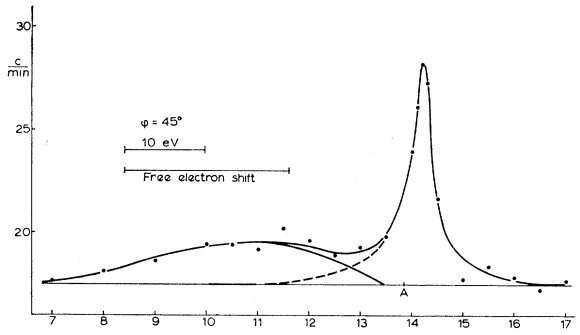


FIG. 8. Scattering on Li. Scattering angle larger than $\varphi_0$.

from the bent crystal remained unchanged. This ensured a large shift of the Compton component, which separated it completely from the Rayleigh line. In Fig. 9 we give the dummy experiment curve for the case of $\varphi=10°$.

## COMPTON PROFILES

If Fig. 9 is plotted along with the Li curve for $\varphi=10°$ (Fig. 5) it will allow us to obtain the Compton profile. This necessitates a reduction of the dummy-experiment curve, which was done in the following way: In both Li and Cr curves we first find the net intensity by subtracting the background. Then we calculate the ratio of the net intensities for each micrometer reading. This is done on the region of the Rayleigh line and on its side towards short wavelengths, because we are sure that this region is free from incoherent scattering. In this region a constant ratio was found, which could then be used as a scale factor, which enables us to plot the dummy-experiment curve on the Li curve. To do this, we divide all the measured intensities of chromium by the scale factor, and we add to them the background

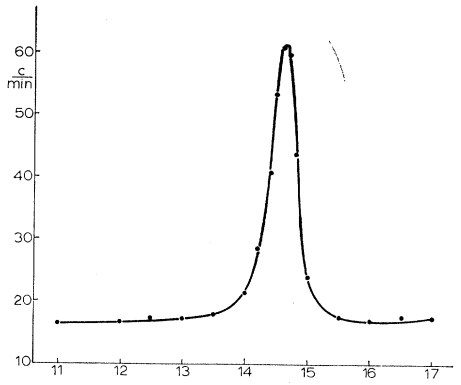


FIG. 9. Experimental curve of fluorescent and scattered radiation from chromium filings ($\varphi=25°$, dummy experiment).

value. The same process was repeated for the other scattering angles ($\varphi=18°$ and 32°) where overlapping occurs. The curves obtained after the reduction are indicated with crosses in Figs. 5 to 7. The Compton intensity for each micrometer reading is found by subtracting the two intensities (Cr from Li). The Compton profile so obtained is plotted for each case underneath the experimental curves (Figs. 5 to 7). In Fig. 8 the two components are sufficiently separated that there was no need for the use of a dummy experiment.

In the "transmission position" of the scatterer, the measurements exhibit similar trends to those in the reflection position, but they do not provide a satisfactory scale factor. Therefore, use was made only of the measurements with the scatterer in the reflection position.

## DISCUSSION OF RESULTS

These measurements were limited to relatively small scattering angles, for which, as is well known, the Compton band is rather narrow. If we take into account the fact that the curve of the unmodified radiation is far from being monochromatic, an "unfolding" of the experimental curves is necessary to allow comparison with the theoretical curves. Unfortunately, because of mathematical complexity, the process based on the Fourier analysis was carried out only for the case of scattering angle $\varphi=10°$. From the smoothed curve of the Compton profile (Fig. 5), the inverse Fourier method[14,15] gave the points marked on Fig. 10. Drawing a smooth curve through these points,

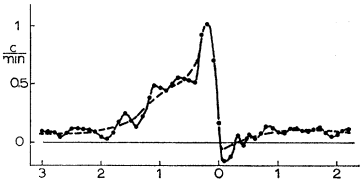


FIG. 10. The Compton profile for $\varphi=10°$ after the "unfolding." Wavelength increasing towards the left. The horizontal axis in mm.

[14] H. Lipson and C. A. Beevers, Proc. Phys. Soc. (London) **48**, 772 (1936).
[15] A. R. Stokes, Proc. Phys. Soc. (London) **61**, 382 (1948).

we can make the following comments: (a) The width of the base seems to be practically unchanged; (b) the side of the curve towards the unmodified line is, as expected, steeper; and (c) the other side of the curve is far from being a section of an inverse parabola as the theory predicts. Under these conditions we can say that the profile does not exhibit the expected shape, calculated by the simple theory, based on the free-electron gas without interaction (Fig. 3).

On the other hand, comparing this curve with the theoretical results by Ohmura and Matsudaira, we also have a disagreement in the general shape of the profile (Fig. 3 in Ref. 8).

All our discussions are based on the smooth curve of Fig. 5. Because the statistical errors allow the choice of a shape that might differ considerably from the one we assume, the above criticism of the theoretical curves is not conclusive. We hope in the future to continue measurements under better conditions, namely by using an x-ray tube of much higher power.

Further, we can say that under the present experimental conditions, the scattering is due only to the valence electrons, since the contribution of the two $K$ electrons of Li is not possible. This is so because the excitation energy of the $K$ electrons is of the order of 54 eV, while in the present work we deal only with much smaller energy transfer.

One of our measurements ($\varphi=45°$, Fig. 8) refers to a scattering angle that is beyond the critical value $\varphi_0$, a case for which, in both theories (i.e., with and without interaction), the profile should be a parabola. The experimental total broadening of the band is 43 eV, while the formula $\delta\lambda=4\lambda(v/c)\sin(\frac{1}{2}\varphi)$, gives the value 39 eV for monochromatic primary radiation and a free-electron gas.

The measured half-width of the Compton band is about 28 eV, the error of which might be of the order of 20%. Neither value is perceptibly influenced by "folding," because the profile of the primary radiation has a half-width of only 3.5 eV.

The half-width of 28±5 eV has to be compared with the theoretical value given by March. From his curve of the Compton profile (Fig. 2, Ref. 3) we take the value $q=0.5$, which corresponds to half the maximum value of $J(q)$. In our case this gives 33 eV.

We notice that, in the region of our measurements, experiment and Hartree-Fock theory agree within experimental errors. In the region of higher energy shifts[7] (~700 eV), the measured half-width exceeds the theoretical value by 30%.

## APPENDIX: CALCULATION OF THE COMPTON PROFILE

Since only the electrons in the shaded part of Fig. 1 contribute to the scattering, we can find the correlation between the shape of the Compton band and the shaded part of the Fermi sphere. To this end, we cut

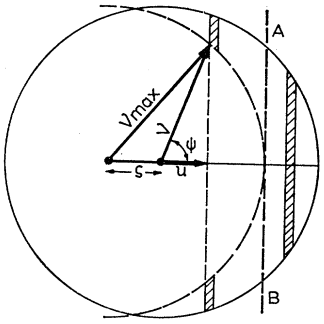


FIG. 11. For the calculation of the Compton profile.

the Compton band in a number of vertical strips of infinitesimal thickness, each of which corresponds to a certain slice cut from the shaded part of the Fermi sphere. We then notice that only those electrons having a component of their momentum parallel to the scattering vector within the range $p$ to $p+dp$ contribute to a given range between $\lambda$ and $\lambda+d\lambda$ in the Compton band. As the density of occupation of the Fermi sphere is constant, the volume of the slices, which can be found by a geometrical computation, is a measure of the number of electrons contributing to the scattering and therefore of the intensity distribution within the Compton band.

The calculation gives the shape $f(x)$ of the band as a function of the wavelength shift $x$ which is measured on both sides from the position of the Compton line (electron at rest). The following calculation is based on the paper by Kappeler.[6] It begins with the calculation of the number of electrons having velocities between $v$ and $v+dv$ and velocity projections from $u$ to $u+du$. (see Fig. 11). These electrons contribute to a certain elementary range in the Compton band, where the intensity is given by the formula

$$df(x)dx=W(v)\frac{2\pi v^2\sin\psi d\psi}{4\pi v^2}dv.$$

$W(v)$ is the velocity distribution and angle $\psi$ locates a certain spherical zone inside the Fermi sphere. Introducing the velocity projection $u=v\cos\psi$ we obtain $df(x)dx=(1/2)W(v)(du/v)dv$. We simplify this formula by using the relation $x=(2\lambda/c)[\sin(\frac{1}{2}\varphi)]u$, which gives the wavelength shift. Then we have

$$df(x)dx=\tfrac{1}{4}W(v)(dx\,c/\lambda\sin(\tfrac{1}{2}\varphi)v)dv,$$

which by integration gives

$$f(x)=\frac{c}{4\lambda\sin(\varphi/2)}\int_{v=u}^{v=v_{\max}}\frac{W(v)}{v}dv.$$

The limits of this integration are easily understood.

We apply[16] this formula to the case of the free-electron gas by introducing the distribution function

$$W(v)=(8\pi m^3/h^3)(V/N)v^2.$$

[16] This application was carried out by A. Nikolitsas.

Then we have

$$f(x)=\frac{8\pi cVm^3}{4\lambda h^3N\sin(\frac{1}{2}\varphi)}\int_{v=u}^{v=v_{\max}}vdv$$

$$=\frac{\pi cVm^3}{\lambda h^3N\sin(\frac{1}{2}\varphi)}(v_{\max}{}^2-u^2)$$

$$=\frac{\pi cVm^3}{\lambda h^3N\sin(\frac{1}{2}\varphi)}\left(v_{\max}{}^2-\frac{c^2}{4\lambda^2\sin^2(\frac{1}{2}\varphi)}x^2\right),$$

where the variable is the wavelength shift $x$. Knowing this relation we can determine the shape of the Compton band. For $x=0$ we have the peak of the parabola. The two ends are obtained by replacing $x$ by $x_m=\pm(2\lambda/c)\sin(\frac{1}{2}\varphi)v_{\max}$. This result is valid for scattering angles larger than $\varphi_0$. For the case of $\varphi<\varphi_0$, the shaded part of Fig. 1 is divided in two parts lying on either side of the plane AB (Fig. 11). The part to the right of this plane gives a section of the parabola mentioned above, while the other part to the left of the plane AB gives a linear section of the profile. Using for the variable $x$ the limits

$$(2\lambda/c)\sin(\tfrac{1}{2}\varphi)(-\tfrac{1}{2}s)\leqslant x\leqslant(2\lambda/c)\sin(\tfrac{1}{2}\varphi)(v_{\max}-s),$$

we find easily

$$f(x)=\frac{\pi cVm^3}{\lambda h^3N\sin(\frac{1}{2}\varphi)}\left(s^2+\frac{sc}{\lambda\sin(\frac{1}{2}\varphi)}x\right),$$

which represent a straight line. On the basis of this calculation we plotted the curve of Fig. 3 for $\varphi=10°$.

## ACKNOWLEDGMENTS

We are greatly indebted to Professor K. Alexopoulos for many stimulating discussions during this work and also for his comments on the manuscript. We express also our gratitude to Dr. C. A. Beevers of Edinburgh University, who drew the curve of Fig. 10 according to his method.

PHYSICAL REVIEW VOLUME 145, NUMBER 2 13 MAY 1966

# Energy and Atomic Configuration of Complete and Dissociated Dislocations. I. Edge Dislocation in an fcc Metal*

R. M. J. Cotterill and M. Doyama
*Argonne National Laboratory, Argonne, Illinois*

(Received 18 September 1964; revised manuscript received 20 December 1965)

The arrangement of atoms around an edge dislocation in copper has been calculated by a variational method using a central-force approximation. The pairwise interaction between discrete atoms was represented by a Morse potential function. In the calculation of the complete dislocation, the atoms were not permitted to relax in a direction parallel to the dislocation line. This prevented dissociation. Linear-elasticity theory is found to break down inside a core radius of 9 Å for a complete ⟨112⟩ dislocation [Burgers vector $=(a_0/2)\langle 110\rangle$, where $a_0$ is the lattice constant]. The corresponding core energy is 0.65 eV per {112} plane. If the core is replaced by a cylindrical hole of radius $r_{eh}$ (the *equivalent hole* radius), the inside of which is hollow and outside of which linear-elastic theory holds at all points, this radius is 0.8 Å. The complete dislocation was found to have a width of 13 Å (i.e., about five Burgers vectors). The core region is found to be neither hollow nor like a liquid. If the atoms are permitted to relax in a direction parallel to the dislocation line, the dislocation spontaneously dissociates into two Heidenreich-Shockley partials; and this process involves no activation energy. A stacking fault of infinite extent has an energy of 30 erg cm$^{-2}$ for the potential and truncation used in the calculation. Certain precautions must be taken to ensure that the separation distance of the partials is the same as the distance given by elastic theory. Several different potential forms were used in the calculations of stacking-fault energy. The stacking-fault energy is found to be critically dependent upon the form of the interatomic potential. For the pseudopotential for aluminum given by Harrison, the stacking-fault energy is approximately 250 erg cm$^{-2}$.

## I. INTRODUCTION

THE elastic-continuum treatment of dislocations in metal crystals has always suffered from difficulties associated with the dislocation core. Expressions for the stresses around a dislocation, derived by the continuum method, invariably have a singularity at the center of the dislocation. It is clear that such a singularity does not occur in a real crystal. This difficulty is usually overcome by treating separately that part of the crystal which lies inside a small cylinderical core whose axis is the dislocation and the radius of which is $r_c$, say. This part is referred to as the dislocation core, and the linear elastic theory is said to break down in this region. The integrations which are involved in calculations of dislocation energy use $r_c$ as a lower limit of

* Based on work performed under the auspices of the U. S. Atomic Energy Commission.